Journal of Computational Mathematics
Vol.xx, No.x, 2025, 1–24.

http://www.global-sci.org/jcm
doi:10.4208/jcm.2502-m2024-0035

A NEW ANALYTICAL STUDY FOR MULTI-DIMENSIONAL NAVIER-STOKES EQUATIONS WITH TIME-FRACTIONAL ORDER*

Hegagi Mohamed Ali
Department of Mathematics, College of Science, University of Bisha, Bisha 61922, Saudi Arabia;
Department of Mathematics, Faculty of Science, Aswan University, Aswan 81528, Egypt
Emails: hegagi_math@aswu.edu.eg, he.ahmed@ub.edu.sa

Abstract

In this research article, we present convenient analytical-approximate solutions for fluid flow models known as multi-dimensional Navier-Stokes equations containing time-fractional order by using a relatively new analytical method called modified generalized Mittag-Leffler function method. The Caputo fractional derivative is used to describe fractional mathematical formalism. The approximate solutions for five problems are implemented to demonstrate the validity and accuracy of the proposed method. It is also demonstrated that the solutions obtained from our method when $\alpha = 1$ coincide with the exact solutions, this is displayed by using some 2D and 3D plots for each problem. Moreover, the comparison between our outcomes with given exact solutions and results obtained by other methods in the literature besides absolute error is provided in some tables. Additionally, we offer some plots when α has different values to present the effect of fractional order on the solution of each suggested problem. The numerical simulation presented in this work indicates that the proposed method is efficient, reliable, accurate and easy which has less computational ability to give analytical-approximate solution form. So, this method can be extended to implement on different related problems arising in various areas of innovation and research.

Mathematics subject classification: 35Q30, 35R11, 33E12, 74H10.
Key words: Navier-Stokes equations, Fractional partial differential equations, Mittag-Leffler function, Nonlinear problems, Analytic approximate solutions.

1. Introduction

The Navier-Stokes equations (NSEs) are considered famous partial differential equations (PDEs) that govern the motion of viscous fluid flow and describe different geophysical fluid mechanical problems. NSEs are the primary PDEs that relate momentum, continuity and energy equations and the first appearance of NSEs in the year 1822 [34]. Then, these equations have been used to describe many various interesting applications in theoretical studies and physical phenomena such as liquid flow in pipes, managing climate estimating, ocean currents, airflow around the wings of aircraft, blood flow and examination of contamination [33, 40].

The first formulation of NSEs in fractional order was done by El-Shahed and Salem [17] in 2005, they solved this model by using finite Fourier Sine transform, finite Hankel transforms and Laplace transform. After that many researchers have tried to solve NSEs by using different methods for example: in [14], authors used the variational iteration transform technique to evaluate multi-dimensional fractional NSEs. In [23], the residual power series method has been

* Received February 19, 2024 / Revised version received September 4, 2024 / Accepted February 17, 2025 / Published online April 7, 2025 /

applied for the solution of the fractional NSEs with 2 and 3 dimensions. In [22], a hybrid approach of decomposition method and Elzaki transformation has been applied to solve fractional NSEs. In [36], authors have adopted a fractional reduced differential transformation method as a semi-analytical scheme to get an approximate solution of fractional NSEs and many other research papers in the literature (see, e.g. [16, 19–21, 25]).

The classical Navier-Stokes and continuity equations are given by

$$\begin{aligned} &\frac{\partial \Theta}{\partial t} + (\Theta \cdot \bigtriangledown)\Theta = K \bigtriangledown^2 \Theta - \frac{1}{\rho} \bigtriangledown P, \\ &\bigtriangledown \cdot \Theta = 0, \\ &\Theta = 0 \quad \text{on } \Omega \times (0, T), \end{aligned} \tag{1.1}$$

where $\Theta = (U, V, W)$ and P represent the fluid vector of velocity and pressure, respectively, ρ is the density, $K = \phi/\rho$ is the kinematics viscosity, ϕ is the dynamic viscosity, (x, y, z) are spatial components in Ω and t is the time variable.

Fractional calculus (FC) is a branch of mathematics concerned with integrals and derivatives of arbitrary orders. Thus, it is considered a generalization of the integer-order calculus. Furthermore, the differential equations whether partial or ordinary that have fractional order are called fractional differential equations (FDEs). Recently, FDEs have acquired popularity, importance and attracted many famous researchers and scientists [9, 31, 38, 39]. This is due to its prominent applications in many fields of science and engineering, such as reaction-diffusion, electric networks, electrochemistry of corrosion, polymer physics, fluid flow, chemical physics, propagation of waves and many other important applications [5, 6, 11–13, 26, 27, 29, 37].

The most advantage of using FC in describing applications is that it predicts the future and gives a good description of the behavior of the system from the integer case due to its properties like non-locality, non-singularity, kernel, memory effect and so on. This means that the fractional models are featured because they do not depend on the current situation, but rather depend on all genetic and historical cases (memory effect).

The main goal and motivation are to investigate on solution of time fractional order multi-dimensional NSEs using modified generalized Mittag-Leffler function method (MGMLFM). The generalization of the classical problem Eq. (1.1) with fractional order $0 < \alpha \leq 1$ is defined as

$$\begin{aligned} &{}_0^C D_t^\alpha \Theta + (\Theta \cdot \bigtriangledown)\Theta = K \bigtriangledown^2 \Theta - \frac{1}{\rho} \bigtriangledown P, \\ &\bigtriangledown \cdot \Theta = 0, \\ &\Theta = 0 \quad \text{on } \Omega \times (0, T), \end{aligned} \tag{1.2}$$

where ${}_0^C D_t^\alpha$ is Caputo fractional derivative (CFD).

The novelty and our contribution to this work are evident in presenting the MGMLFM as an analytical technique to give the appropriate solution for multi-dimensional NSEs within fractional order. The analytical solutions for five different problems of fractional NSEs are calculated by using the proposed method. The obtained results are displayed and verified with some 2D and 3D plots for each problem. Moreover, the comparison of these outcomes with given exact solutions and others obtained by different techniques in the literature besides absolute error is provided in some tables to show the validity and accuracy of the MGMLFM. The solution to these illustrative problems proved that the MGMLFM has less computing costs, straightforward steps and higher convergence rates. Therefore, the MGMLFM is constructive to

solving other fractional linear and nonlinear PDEs which describes a lot of problems in various fields of applied sciences.

The outline of this paper is prepared as follows. Section 2 provides some fundamental principles for FC in order to progress in this research work. In Section 3, we constructed the general algorithm of the MGMLFM to give a solution of nonlinear fractional PDEs. Section 4 is devoted to implementing the proposed method on fractional multi-dimensional NSEs, five interesting examples are considered to demonstrate the simplicity and accuracy of MGMLFM. Also, the simulation of the outcomes displayed in figures and tables is presented in this section. In Section 5, we draw the conclusion of this work.

2. Preliminaries

Here, some important concepts and definitions of FC are presented to accomplish this work [10, 24, 35].

Definition 2.1. *For a function $\Phi(\xi,t)$ and $t\in[0,T]$, the fractional order Riemann-Liouville integral is*

$$ {}_0I_t^{\alpha}\Phi(\xi,t)=\begin{cases}\dfrac{1}{\Gamma(\alpha)}\displaystyle\int_0^t(t-\tau)^{\alpha-1}\Phi(\xi,\tau)d\tau, & \alpha>0,\quad t>0,\\ \Phi(\xi,t), & \alpha=0.\end{cases}$$

Definition 2.2. *The CFD for absolutely continuous function $\Phi(\xi,t)$ on $[0,T]$ is*

$$ {}_0^CD_t^{\alpha}\Phi(\xi,t)=\begin{cases}\dfrac{1}{\Gamma(n-\alpha)}\displaystyle\int_0^t(t-\tau)^{n-\alpha-1}\frac{\partial^n\Phi(\xi,\tau)}{\partial\tau^n}d\tau, & \text{if}\quad n-1<\alpha<n,\quad n\in\mathbb{N},\quad t>0,\\ \dfrac{\partial^n\Phi(\xi,t)}{\partial t^n}, & \text{if}\quad \alpha=n,\quad n\in\mathbb{N},\end{cases}$$

when $n=1$, we have

$$ {}_0^CD_t^{\alpha}\Phi(\xi,t)=\frac{1}{\Gamma(1-\alpha)}\int_0^t(t-\tau)^{-\alpha}\frac{\partial\Phi(\xi,\tau)}{\partial\tau}d\tau,\quad t>0,\quad 0<\alpha<1.$$

Theorem 2.1. *Let $\Phi(\xi,t)$ is a differentiable function, $t\in[0,T]$ and $\alpha\in(n-1,n], n\in\mathbb{N}$, then*

$$ {}_0^CD_t^{\alpha}\,{}_0I_t^{\alpha}\Phi(\xi,t)=\Phi(\xi,t),$$
$$ {}_0I_t^{\alpha}\,{}_0^CD_t^{\alpha}\Phi(\xi,t)=\Phi(\xi,t)-\sum_{k=0}^{n-1}\frac{\partial^k\Phi(\xi,t)}{\partial t^k}\Big|_{t=0}\frac{t^k}{k!}.$$

Moreover, for $\gamma>-1$ we have

$$ {}_0^CD_t^{\alpha}t^{\gamma}=\frac{\Gamma(\gamma+1)}{\Gamma(\gamma-\alpha+1)}t^{\gamma-\alpha},\quad {}_0I_t^{\alpha}t^{\gamma}=\frac{\Gamma(\gamma+1)}{\Gamma(\gamma+\alpha+1)}t^{\gamma+\alpha}.$$

Definition 2.3. *The Mittag-Leffler function is defined by*

$$ E_{\alpha}(z)=\sum_{n=0}^{\infty}\frac{z^n}{\Gamma(n\alpha+1)},\quad \alpha>0,\quad z\in\mathbb{C}.$$

Lemma 2.1. *The fractional derivative of the generalized Mittag-Leffler function in Caputo sense is given as*

$$ {}_0^C D_t^\alpha E_\alpha(\lambda t^\alpha) = {}_0^C D_t^\alpha \left(\sum_{n=0}^{\infty} \frac{\lambda^n t^{n\alpha}}{\Gamma(n\alpha+1)} \right) = \sum_{n=1}^{\infty} \frac{\lambda^n t^{(n-1)\alpha}}{\Gamma\big((n-1)\alpha+1\big)} = \sum_{n=0}^{\infty} \frac{\lambda^{n+1} t^{n\alpha}}{\Gamma(n\alpha+1)} = \lambda E_\alpha(\lambda t^\alpha). $$

Theorem 2.2 ([18]). *Suppose that*

$$ \Phi(\xi,t) = \sum_{k=0}^{\infty} \zeta^k \Phi_k(\xi,t) $$

is a given function and $\mathcal{N}(\cdot)$ is a nonlinear operator. Then, we have

$$ \frac{\partial^n}{\partial \zeta^n} \mathcal{N}(\Phi)|_{\zeta=0} = \frac{\partial^n}{\partial \zeta^n} \mathcal{N} \sum_{k=0}^{\infty} \zeta^k \Phi_k|_{\zeta=0} = \frac{\partial^n}{\partial \zeta^n} \mathcal{N} \sum_{k=0}^{n} \zeta^k \Phi_k|_{\zeta=0}. $$

3. Analysis of the MGMLFM

In this section, we give the algorithm of MGMLFM to provide a general solution for the next time-fractional nonlinear PDEs

$$ {}_0^C D_t^\alpha \Psi(\chi,t) = \mathcal{L}\big(\Psi(\chi,t)\big) + \mathcal{N}\big(\Psi(\chi,t)\big), \tag{3.1} $$

subject to initial conditions (ICs)

$$ \Psi(\chi,0) = \Theta(\chi), \tag{3.2} $$

where

$$ \Psi = \begin{bmatrix} \Psi_1 \\ \Psi_2 \\ \vdots \\ \Psi_m \end{bmatrix}, \quad \chi = \begin{bmatrix} \chi_1 & \chi_2 & \cdots & \chi_n \end{bmatrix}, \quad n,m \in \mathbb{N}, \quad \Theta(\chi) = \begin{bmatrix} \Theta_1 \\ \Theta_2 \\ \vdots \\ \Theta_m \end{bmatrix}, $$

and $\mathcal{L}, \mathcal{N}$ are linear and nonlinear operators.

Based on the previous algorithm, the MGMLFM assumed that the solution of $\Psi(\chi,t)$ for Eq. (3.1) is set as

$$ \begin{aligned} \Psi_1(\chi,t) &= \Upsilon_1(\chi) E_\alpha\big(\Lambda_1 t^\alpha\big) = \sum_{k=0}^{\infty} \Upsilon_1(\chi) \Lambda_1^k \frac{t^{k\alpha}}{\Gamma(k\alpha+1)}, \\ \Psi_2(\chi,t) &= \Upsilon_2(\chi) E_\alpha\big(\Lambda_2 t^\alpha\big) = \sum_{k=0}^{\infty} \Upsilon_2(\chi) \Lambda_2^k \frac{t^{k\alpha}}{\Gamma(k\alpha+1)}, \\ &\cdots\cdots \\ \Psi_m(\chi,t) &= \Upsilon_m(\chi) E_\alpha\big(\Lambda_m t^\alpha\big) = \sum_{k=0}^{\infty} \Upsilon_m(\chi) \Lambda_m^k \frac{t^{k\alpha}}{\Gamma(k\alpha+1)}, \end{aligned} \tag{3.3} $$

where $\Lambda_1, \Lambda_2, \ldots, \Lambda_m$ are unidentified coefficients and $\Upsilon_1, \Upsilon_2, \ldots, \Upsilon_m$ are auxiliary functions satisfies $\Upsilon_1 = \Theta_1, \Upsilon_2 = \Theta_2, \ldots, \Upsilon_m = \Theta_m$. Therefore, by utilizing Lemma 2.1 and Eq. (3.3)

the fractional PDE (3.1) is specified by

$$\sum_{k=0}^{\infty}\Theta(\chi)\Lambda_m^{k+1}\frac{t^{k\alpha}}{\Gamma(k\alpha+1)}$$
$$=\mathcal{L}\left(\sum_{k=0}^{\infty}\Theta(\chi)\Lambda_m^{k}\frac{t^{k\alpha}}{\Gamma(k\alpha+1)}\right)+\mathcal{N}\left(\sum_{k=0}^{\infty}\Theta(\chi)\Lambda_m^{k}\frac{t^{k\alpha}}{\Gamma(k\alpha+1)}\right),\quad m\geq 1. \tag{3.4}$$

Consequently, the linear part $\mathcal{L}(\cdot)$ can be written as

$$\mathcal{L}\big(\Psi(\chi,t)\big)=\mathcal{L}\left(\sum_{k=0}^{\infty}\Theta(\chi)\Lambda_m^{k}\frac{t^{k\alpha}}{\Gamma(k\alpha+1)}\right)=\sum_{k=0}^{\infty}\mathcal{L}\left(\Theta(\chi)\Lambda_m^{k}\frac{t^{k\alpha}}{\Gamma(k\alpha+1)}\right). \tag{3.5}$$

According to He's polynomials [18,32] and the Theorem 2.2 the nonlinear part $\mathcal{N}(\cdot)$ is given as

$$\mathcal{N}\big(\Psi(\chi,t)\big)=\mathcal{N}\left(\sum_{k=0}^{\infty}\Theta(\chi)\Lambda_m^{k}\frac{t^{k\alpha}}{\Gamma(k\alpha+1)}\right)=\sum_{k=0}^{\infty}\mathcal{N}\big(\Theta(\chi)\Psi_k(\chi,t)\big)$$
$$=\mathcal{N}\big(\Theta(\chi)\big)\left(N\big(\Psi_0(\chi,t)\big)+\sum_{k=1}^{\infty}\mathcal{N}\left(\sum_{i=0}^{k}\Psi_i(\chi,t)\right)-\mathcal{N}\left(\sum_{i=0}^{k-1}\Psi_i(\chi,t)\right)\right). \tag{3.6}$$

Replacing linear and nonlinear parts from Eq. (3.4) by Eqs. (3.5) and (3.6), we acquire a recurrence relation to recognize the coefficients Λ_m. Therefore, we gain a solution of Eq. (3.1). To check the convergence of the Mittag-Leffler function you can review [1–3, 7, 8, 28, 30].

Regarding the error estimator and convergence of the given algorithm, we offer the following theorem.

Theorem 3.1. *Suppose that $H=L^2((\epsilon,\eta)\times[0,T])$ is a Hilbert space with the related norm*

$$\|\digamma^2\|=\int_{(\epsilon,\eta)\times[0,T]}\digamma^2(x,\lambda)\;d\lambda\;d\tau<+\infty,$$

and the following two hypotheses $\mathcal{H}_1,\mathcal{H}_2$ are satisfied:

($\mathcal{H}_1$) $(\psi(\digamma_1)-\psi(\digamma_2),\digamma_1-\digamma_2)\geq K\|\digamma_1-\digamma_2\|^2;\ K>0,\ \digamma_1,\digamma_2\in H.$

($\mathcal{H}_2$) *Whenever a constant $\varrho>0$, then there exist $M(\varrho)>0$, since $\|\digamma_1\|\leq\varrho,\|\digamma_2\|\leq\varrho$, for any $\digamma_1,\digamma_2\in H$ and we have*

$$\big(\psi(\digamma_1)-\psi(\digamma_2),\omega\big)\leq M(\varrho)\|\digamma_1-\digamma_2\|\|\omega\|,\quad\forall\,\omega\in H,$$

where the operator $\psi(\digamma_1)$ following Eq. (3.1) *is given by*

$$\psi(\digamma_1)={}^{C}D_t^{\alpha}\digamma_1(x,t)=L\big(\digamma_1(x,t)\big)+N\big(\digamma_1(x,t)\big).$$

Then, the MGMLFM is convergence.

Proof. The proof can be processed in the same manner in [4, 15]. □

4. Application and Results

Problem 4.1. Consider the one-dimensional time fractional-order NSE

$$ {}_0^C D_t^\alpha U(x,t) = p + \frac{\partial^2 U(x,t)}{\partial x^2} + \frac{1}{x}\frac{\partial U(x,t)}{\partial x}, \quad 0 < \alpha \leq 1 \tag{4.1} $$

with the initial condition

$$ U(x,0) = U_0 = 1 - x^2, \tag{4.2} $$

where

$$ p = -\frac{1}{\rho}\frac{\partial P}{\partial x} = 1. $$

As a special case when $\alpha = 1$, then the exact solution [25] is given by

$$ U(x,t) = 1 - x^2 + (p-4)t. \tag{4.3} $$

To apply the MGMLFM, we assume the approximate solution of Eq. (4.1) as the following:

$$ U(x,t) = \Upsilon(x) E_\alpha(\Lambda t^\alpha) = \sum_{k=0}^{\infty} \Upsilon(x) \Lambda^k \frac{t^{k\alpha}}{\Gamma(k\alpha+1)}. \tag{4.4} $$

Following the same approach in Section 3, we get

$$ \sum_{n=0}^{\infty} \left(U_0 \Lambda^{n+1} - \frac{\partial^2 \big(U_0 \Lambda^n\big)}{\partial x^2} - \frac{1}{x}\frac{\partial \big(U_0 \Lambda^n\big)}{\partial x} \right) \frac{t^{n\alpha}}{\Gamma(n\alpha+1)} = p. $$

For $n = 0$, we have

$$ \Lambda^1 = \frac{1}{U_0}\left(p + \frac{\partial^2 \big(U_0 \Lambda^0\big)}{\partial x^2} + \frac{1}{x}\frac{\partial \big(U_0 \Lambda^0\big)}{\partial x} \right) = p - 4. $$

Then, for $n \geq 1$ we have the following recurrence relation:

$$ \Lambda^{n+1} = \frac{1}{U_0}\left(p + \frac{\partial^2 \big(U_0 \Lambda^n\big)}{\partial x^2} + \frac{1}{x}\frac{\partial \big(U_0 \Lambda^n\big)}{\partial x} \right). \tag{4.5} $$

After replacing various values of $n = 1, 2, \ldots$, we have $\Lambda^2, \Lambda^3, \Lambda^4, \ldots$ to get the following fractional approximate solution:

$$ U(x,t) = U_0 \left(\Lambda^0 + \Lambda^1 \frac{t^\alpha}{\Gamma(\alpha+1)} + \Lambda^2 \frac{t^{2\alpha}}{\Gamma(2\alpha+1)} + \Lambda^3 \frac{t^{3\alpha}}{\Gamma(3\alpha+1)} + \cdots \right). $$

The numerical simulation for this problem is displayed in Figs. 4.1-4.3, where the comparison between the obtained approximate solution when $\alpha = 1$ with the exact solution is shown in Fig. 4.1 beside the associated absolute error to show how well our output matches the exact solution. In Fig. 4.2, we show the behavior of fractional order solutions for various values of $\alpha = 0.9, 0.8$ and 0.7. In Fig. 4.3, we present 2D plots for the obtained solution with respect to t and x in Fig. 4.3(a) and 4.3(b), respectively, when α takes various values compared with the exact solution. From these figures, it appears that the approximate solution is completely compatible with the given exact solution.

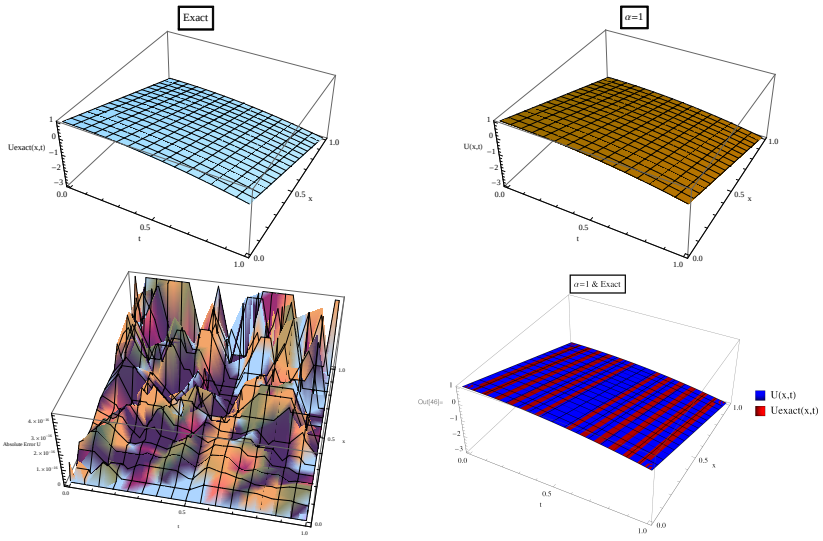

Fig. 4.1. The MGMLFM solution of $U(x,t)$ when $\alpha = 1$, exact solution and absolute errors for Problem 4.1.

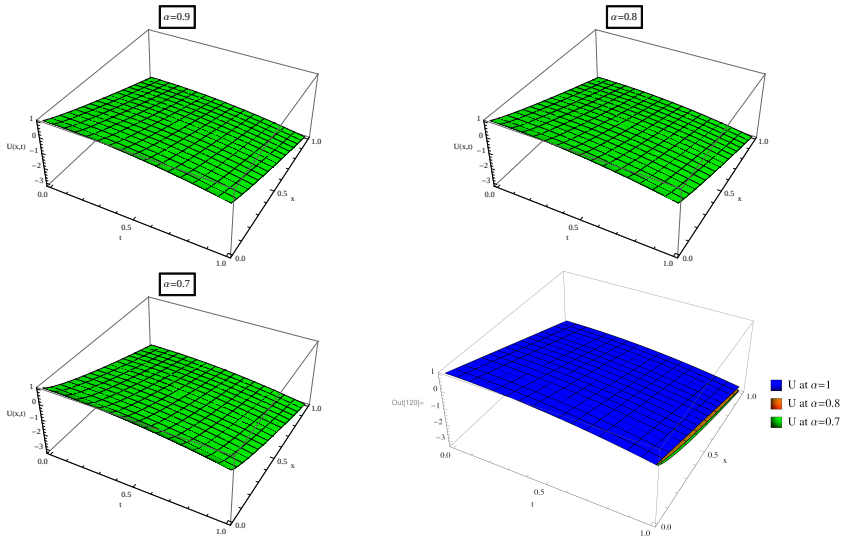

Fig. 4.2. The MGMLFM solution of $U(x,t)$ for Problem 4.1 with various values of α.

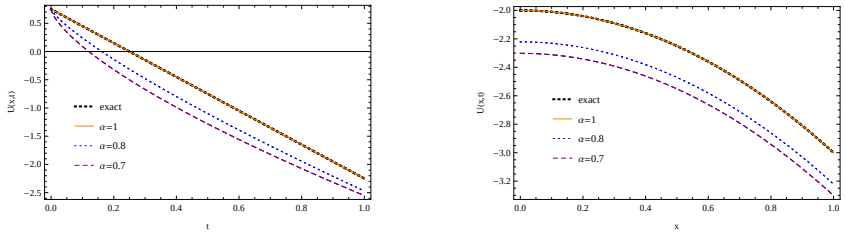

(a) (b)

Fig. 4.3. The MGMLFM solution of $U(x,t)$ for Problem 4.1 when α takes different values, (a) with t and (b) with x .

Problem 4.2. Consider the one-dimensional time fractional-order NSE

$$ {}_0^C D_t^\alpha U(x,t) = \frac{\partial^2 U(x,t)}{\partial x^2} + \frac{1}{x}\frac{\partial U(x,t)}{\partial x}, \quad 0 < \alpha \leq 1 \tag{4.6} $$

with the initial condition

$$ U(x,0) = U_0 = x. \tag{4.7} $$

By setting $\alpha = 1$, we have the following exact solution [25]:

$$ U(x,t) = x + \sum_{m=1}^{\infty} \frac{1^2 \times 3^2 \times \cdots \times (2m-3)^2}{x^{2m-1}} \frac{t^m}{m!}. \tag{4.8} $$

In the same manner as in Problem 4.1, we suggest the approximate solution of Eq. (4.6) as in Eq. (4.4). Therefore Eq. (4.6) becomes in the following form:

$$ \sum_{n=0}^{\infty} \left(U_0 \Lambda^{n+1} - \frac{\partial^2 \left(U_0 \Lambda^n\right)}{\partial x^2} - \frac{1}{x}\frac{\partial \left(U_0 \Lambda^n\right)}{\partial x} \right) \frac{t^{n\alpha}}{\Gamma(n\alpha+1)} = 0. $$

Then, the recurrence relation is as follows:

$$ \Lambda^{n+1} = \frac{1}{U_0}\left(\frac{\partial^2 (U_0 \Lambda^n)}{\partial x^2} + \frac{1}{x}\frac{\partial (U_0 \Lambda^n)}{\partial x} \right). \tag{4.9} $$

By substituting various values of $n = 0, 1, 2, \ldots$, we get the coefficients $\Lambda^1, \Lambda^2, \Lambda^3, \ldots$ to get the following fractional approximate solution:

$$ U(x,t) = U_0 \left(\Lambda^0 + \Lambda^1 \frac{t^\alpha}{\Gamma(\alpha+1)} + \Lambda^2 \frac{t^{2\alpha}}{\Gamma(2\alpha+1)} + \Lambda^3 \frac{t^{3\alpha}}{\Gamma(3\alpha+1)} + \cdots \right). $$

The simulation for this problem is depicted in Figs. 4.4 and 4.5, where the comparison between the approximate solution obtained by MGMLFM when $\alpha = 1$ with the known exact solution (4.8) is presented in Fig. 4.4 alongside the associated absolute error to demonstrate that our results have excellent agreement with the given exact solution. Moreover, the influence of α on the obtained approximate solution is shown in Fig. 4.5.

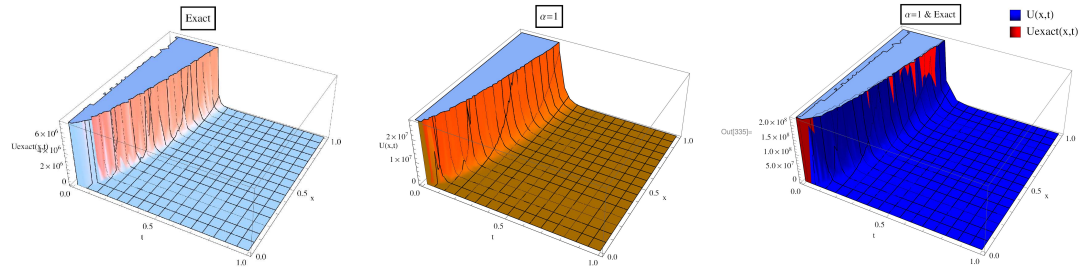

Fig. 4.4. The MGMLFM approximate solution of $U(x,t)$ when $\alpha = 1$, exact solution and absolute errors for Problem 4.2.

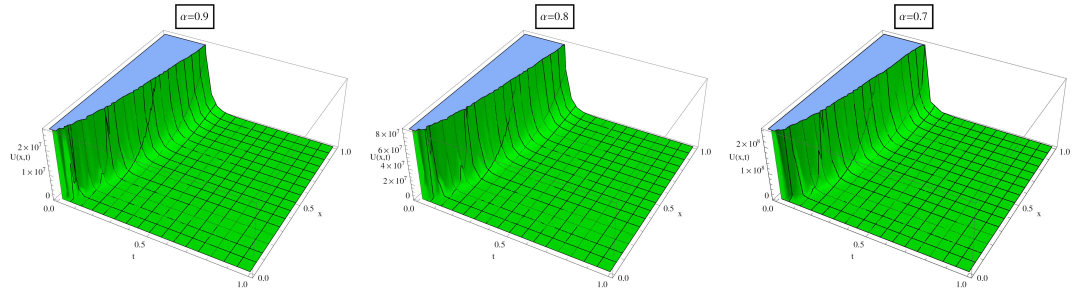

Fig. 4.5. The MGMLFM approximate solutions of $U(x,t)$ for Problem 4.2 with different values of α.

Problem 4.3. Consider the two-dimensional time fractional-order NSEs

$$\begin{aligned}
&{}_0^C D_t^\alpha U(x,y,t) + U(x,y,t)\frac{\partial U(x,y,t)}{\partial x} + V(x,y,t)\frac{\partial U(x,y,t)}{\partial y} \\
&= K\left[\frac{\partial^2 U(x,y,t)}{\partial x^2} + \frac{\partial^2 U(x,y,t)}{\partial y^2}\right] + P, \\
&{}_0^C D_t^\alpha V(x,y,t) + U(x,y,t)\frac{\partial V(x,y,t)}{\partial x} + V(x,y,t)\frac{\partial V(x,y,t)}{\partial y} \\
&= K\left[\frac{\partial^2 V(x,y,t)}{\partial x^2} + \frac{\partial^2 V(x,y,t)}{\partial y^2}\right] - P
\end{aligned} \tag{4.10}$$

with the associated ICs

$$U(x,y,0) = -\sin(x+y) = U_0, \quad V(x,y,0) = \sin(x+y) = V_0. \tag{4.11}$$

In the particular case when $\alpha = 1$, the exact solution [14, 22] is given by

$$U(x,y,t) = -e^{-2Kt}\sin(x+y), \quad V(x,y,t) = e^{-2Kt}\sin(x+y). \tag{4.12}$$

Following the analysis of the MGMLFM presented in Section 3, we assume that the solution of Eq. (4.3) is given by

$$\begin{aligned}
U(x,y,t) &= \Upsilon_1(x,y)E_\alpha\left(\Lambda_1 t^\alpha\right) = \sum_{n=0}^{\infty}\Upsilon_1(x,y)\Lambda_1^n\frac{t^{n\alpha}}{\Gamma(n\alpha+1)}, \\
V(x,y,t) &= \Upsilon_2(x,y)E_\alpha\left(\Lambda_2 t^\alpha\right) = \sum_{n=0}^{\infty}\Upsilon_2(x,y)\Lambda_2^n\frac{t^{n\alpha}}{\Gamma(n\alpha+1)},
\end{aligned} \tag{4.13}$$

where Λ_1 and Λ_2 are undetermined coefficients. From Eq. (4.11) we have $\Upsilon_1(x,y) = U_0$ and $\Upsilon_2(x,y) = V_0$.

Thus, by using CFD presented in Lemma 2.1 and suggested approximate solutions in Eq. (4.13), we can rewrite Eq. (4.10) as follows:

$$\begin{aligned}
&\sum_{n=0}^{\infty}\bigg(U_0\Lambda_1^{n+1}+U_0C^n\Gamma(n\alpha+1)+V_0d^n\Gamma(n\alpha+1)\\
&\qquad -K\frac{\partial^2\big(U_0\Lambda_1^n\big)}{\partial x^2}-K\frac{\partial^2\big(U_0\Lambda_1^n\big)}{\partial y^2}\bigg)\frac{t^{n\alpha}}{\Gamma(n\alpha+1)}=P,\\
&\sum_{n=0}^{\infty}\bigg(V_0\Lambda_2^{n+1}+U_0M^n\Gamma(n\alpha+1)+V_0L^n\Gamma(n\alpha+1)\\
&\qquad -K\frac{\partial^2\big(V_0\Lambda_2^n\big)}{\partial x^2}-K\frac{\partial^2\big(V_0\Lambda_2^n\big)}{\partial y^2}\bigg)\frac{t^{n\alpha}}{\Gamma(n\alpha+1)}=-P,
\end{aligned}\tag{4.14}$$

where

$$\begin{aligned}
C^n&=\sum_{k=0}^{n}\frac{\Lambda_1^k\partial\big(U_0\Lambda_1^{n-k}\big)/\partial x}{\Gamma(k\alpha+1)\Gamma\big((n-k)\alpha+1\big)},\\
d^n&=\sum_{k=0}^{n}\frac{\Lambda_2^k\partial\big(U_0\Lambda_1^{n-k}\big)/\partial y}{\Gamma(k\alpha+1)\Gamma\big((n-k)\alpha+1\big)},\\
M^n&=\sum_{k=0}^{n}\frac{\Lambda_1^k\partial\big(V_0\Lambda_2^{n-k}\big)/\partial x}{\Gamma(k\alpha+1)\Gamma\big((n-k)\alpha+1\big)},\\
L^n&=\sum_{k=0}^{n}\frac{\Lambda_2^k\partial\big(V_0\Lambda_2^{n-k}\big)/\partial y}{\Gamma(k\alpha+1)\Gamma\big((n-k)\alpha+1\big)}.
\end{aligned}$$

When $n=0$, we have

$$\begin{aligned}
\Lambda_1^1&=\frac{1}{U_0}\bigg(P+K\bigg[\frac{\partial^2\big(U_0\Lambda_1^0\big)}{\partial x^2}+\frac{\partial^2\big(U_0\Lambda_1^0\big)}{\partial y^2}\bigg]-\big[U_0C^0-V_0d^0\big]\bigg),\\
\Lambda_2^1&=\frac{1}{V_0}\bigg(-P+K\bigg[\frac{\partial^2\big(V_0\Lambda_2^0\big)}{\partial x^2}+\frac{\partial^2\big(V_0\Lambda_2^0\big)}{\partial y^2}\bigg]-\big[U_0M^0-V_0L^0\big]\bigg).
\end{aligned}$$

For $n\geq 1$, the recursive relations are given by

$$\begin{aligned}
\Lambda_1^{n+1}&=\frac{1}{U_0}\bigg(K\bigg[\frac{\partial^2\big(U_0\Lambda_1^n\big)}{\partial x^2}+\frac{\partial^2\big(U_0\Lambda_1^n\big)}{\partial y^2}\bigg]-\big[U_0C^n-V_0d^n\big]\Gamma(n\alpha+1)\bigg),\\
\Lambda_2^{n+1}&=\frac{1}{V_0}\bigg(K\bigg[\frac{\partial^2\big(V_0\Lambda_2^n\big)}{\partial x^2}+\frac{\partial^2\big(V_0\Lambda_2^n\big)}{\partial y^2}\bigg]-\big[U_0M^n-V_0L^n\big]\Gamma(n\alpha+1)\bigg).
\end{aligned}\tag{4.15}$$

We can determine the coefficients Λ_1^{n+1} and Λ_2^{n+1} by replacing $n=1,2,3,\ldots$. After that, we substitute the obtained coefficients in order to have the following approximate solution:

$$\begin{aligned}
U(x,y,t)&=U_0\bigg(\Lambda_1^0+\Lambda_1^1\frac{t^\alpha}{\Gamma(\alpha+1)}+\Lambda_1^2\frac{t^{2\alpha}}{\Gamma(2\alpha+1)}+\Lambda_1^3\frac{t^{3\alpha}}{\Gamma(3\alpha+1)}+\cdots\bigg),\\
V(x,y,t)&=V_0\bigg(\Lambda_2^0+\Lambda_2^1\frac{t^\alpha}{\Gamma(\alpha+1)}+\Lambda_2^2\frac{t^{2\alpha}}{\Gamma(2\alpha+1)}+\Lambda_2^3\frac{t^{3\alpha}}{\Gamma(3\alpha+1)}+\cdots\bigg).
\end{aligned}$$

The numerical simulations of the Problem 4.3 with given ICs in Eq. (4.11) are listed in Figs. 4.6-4.11. In Figs. 4.6 and 4.8, a comparison is presented for the obtained approximate solution by MGMLFM and the exact solution for components $U(x,y,t)$ and $V(x,y,t)$, respectively, for the system (4.10) at $\alpha=1$ with an indication of the absolute error between them.

The graphics indicate the extent of agreement between the approximate solution and the known exact solution, and the small absolute error between them, which confirms the efficiency of the used method. In Figs. 4.7 and 4.9, we display the effect of $\alpha = 0.9, 0.8, 0.7$ on the behavior of the approximate solution for variables $U(x, y, t)$ and $V(x, y, t)$, respectively. These figures confirm the consistency in the behavior of the solution at different values of α. In Figs. 4.10 and 4.11, we give 2D plots of the approximate solution for $U(x, y, t)$ and $V(x, y, t)$ of the system (4.10) with respect to x and t variables, respectively, when α takes various values. Furthermore, Tables 4.1 and 4.2 provided the numerical values of approximate solutions of $U(x, y, t)$ and $V(x, y, t)$ for the system (4.10), respectively. These tables represent a comparison between our obtained approximate solutions by MGMLFM, given exact solutions and the approximate solutions obtained by Elzaki transformation and decomposition method (ETDM) [22], as well as analysis error (i.e. absolute error) for our method and ETDM. These presented results show that the analysis error of our method is much less than the error of the other method (i.e. ETDM), which confirms the efficiency and accuracy of MGMLFM.

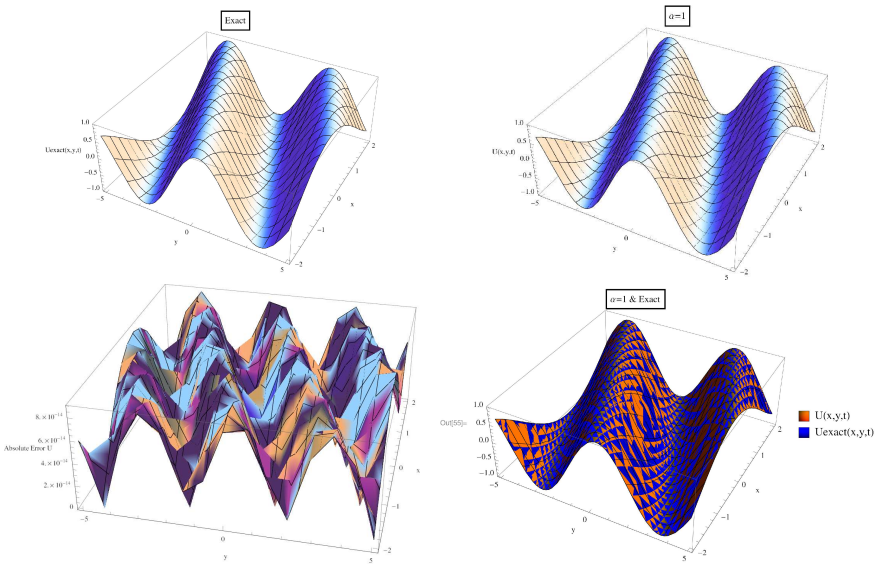

Fig. 4.6. The MGMLFM approximate solution of $U(x, y, t)$ when $\alpha = 1$, exact solution and absolute errors for Problem 4.3.

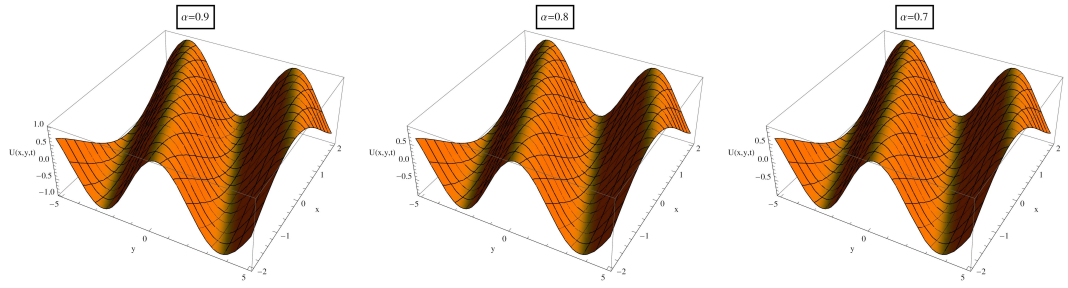

Fig. 4.7. The MGMLFM approximate solutions of $U(x, y, t)$ for Problem 4.3 with different values of α.

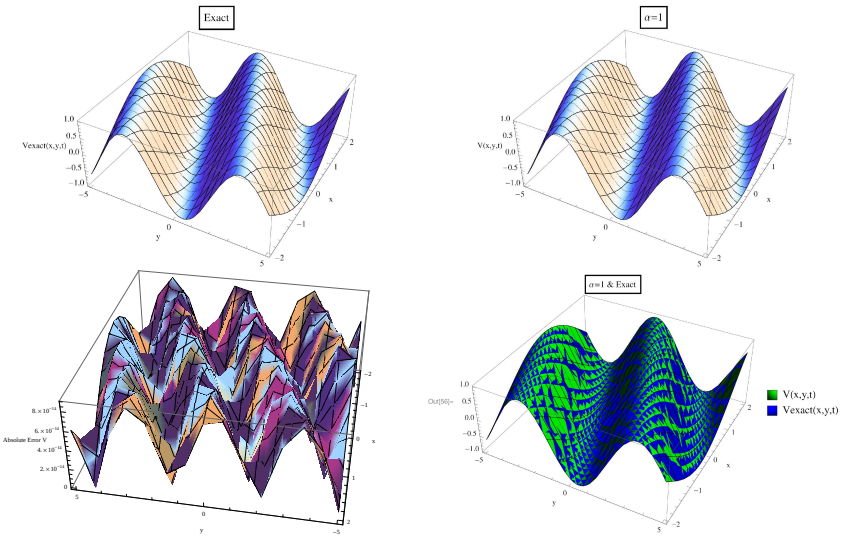

Fig. 4.8. The MGMLFM approximate solution of $V(x, y, t)$ when $\alpha = 1$, exact solution and absolute errors for Problem 4.3.

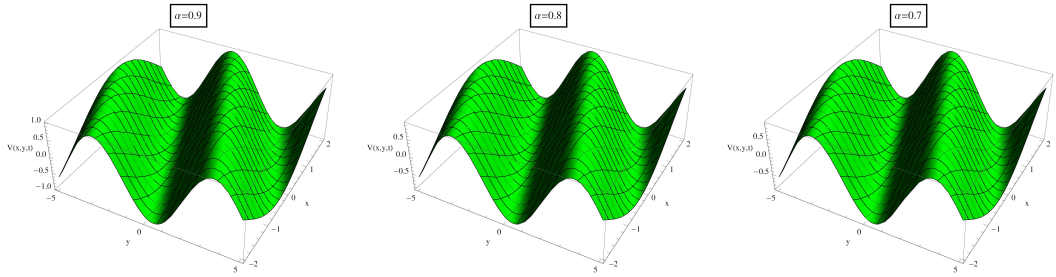

Fig. 4.9. The MGMLFM approximate solutions of $V(x, y, t)$ for Problem 4.3 with different values of α.

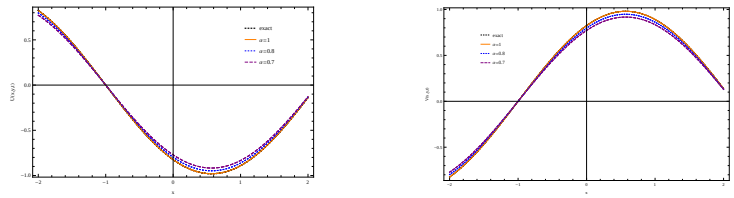

Fig. 4.10. The MGMLFM approximate solutions for $U(x, y, t)$ and $V(x, y, t)$ with x of Problem 4.3, when α takes various values, $y = 1$ and $t = 0.01$.

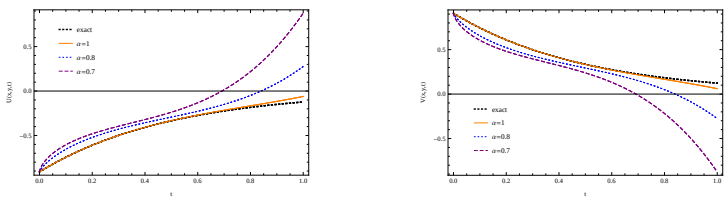

Fig. 4.11. The MGMLFM approximate solutions for $U(x, y, t)$ and $V(x, y, t)$ with t of Problem 4.3, when α takes various values, $y = 1$ and $x = 1$.

Table 4.1: The comparison of the exact and outcomes gained by MGMLFM, ETDM and absolute errors of these methods when $\alpha = 1$ for $U(x, y, t)$ of Problem 4.3 with different values of x at $t = 0.01$ and $y = 1$.

x	Exact	MGMLFM	ETDM [22]
0	−0.824808742934829	−0.8248087429347544	−0.824808737600000
1	−0.8912921314157796	−0.891292131415699	−0.891292125700000
2	−0.13832564467732045	−0.13832564467730796	−0.138325643800000
3	0.7418168018560731	0.7418168018560061	0.741816797100000
4	0.9399363018264509	0.9399363018263659	0.939936295800000
5	0.2738827006359332	0.2738827006359084	0.273882698900000
6	−0.6439773924444746	−0.6439773924444164	−0.643977388300000
7	−0.9697676407653364	−0.9697676407652488	−0.969767634500000
8	−0.4039579924791594	−0.4039579924791229	−0.403957989800000
9	0.5332487711446274	0.5332487711445792	0.533248767700000
10	0.9801890737807477	0.9801890737806591	0.980189067500000
x	Error for ETDM [22]	Error for MGMLFM	
0	$5.3012672040\times10^{-9}$	$7.460698725481052\times10^{-14}$	
1	$5.7285737890\times10^{-9}$	$8.060219158778636\times10^{-14}$	
2	$8.8905605100\times10^{-10}$	$1.249000902703301\times10^{-14}$	
3	$4.7678557200\times10^{-9}$	$6.705747068735946\times10^{-14}$	
4	$6.0412229310\times10^{-9}$	$8.504308368628699\times10^{-14}$	
5	$1.7603176390\times10^{-9}$	$2.475797344914099\times10^{-14}$	
6	$4.1390155720\times10^{-9}$	$5.81756864903582\times10^{-14}$	
7	$6.2329569540\times10^{-9}$	$8.759659664292485\times10^{-14}$	
8	$2.5963464570\times10^{-9}$	$3.652633751016765\times10^{-14}$	
9	$3.4273329990\times10^{-9}$	$4.818367926873179\times10^{-14}$	
10	$6.2999383020\times10^{-9}$	$8.85957973650875\times10^{-14}$	

Problem 4.4. Consider the two-dimensional time fractional-order NSE

$$\begin{aligned} &{}_0^C D_t^\alpha U(x,y,t) + U(x,y,t)\frac{\partial U(x,y,t)}{\partial x} + V(x,y,t)\frac{\partial U(x,y,t)}{\partial y} \\ &= K\left[\frac{\partial^2 U(x,y,t)}{\partial x^2} + \frac{\partial^2 U(x,y,t)}{\partial y^2}\right] + P, \\ &{}_0^C D_t^\alpha V(x,y,t) + U(x,y,t)\frac{\partial V(x,y,t)}{\partial x} + V(x,y,t)\frac{\partial V(x,y,t)}{\partial y} \\ &= K\left[\frac{\partial^2 V(x,y,t)}{\partial x^2} + \frac{\partial^2 V(x,y,t)}{\partial y^2}\right] - P \end{aligned} \tag{4.16}$$

with the associated ICs

$$U(x,y,0) = U_0 = -e^{x+y}, \quad V(x,y,0) = V_0 = e^{x+y}. \tag{4.17}$$

By setting $\alpha = 1$, we have the following exact solution [14, 22]:

$$U(x,y,t) = -e^{x+y+2Kt}, \quad V(x,y,t) = e^{x+y+2Kt}. \tag{4.18}$$

Table 4.2: The comparison of the exact and outcomes gained by MGMLFM, ETDM and absolute errors of these methods when $\alpha = 1$ for $V(x, y, t)$ of Problem 4.3 with various values of x at $t = 0.01$ and $y = 1$.

x	Exact	MGMLFM	ETDM [22]
0	0.824808742934829	0.8248087429347544	0.824808737600000
1	0.8912921314157796	0.891292131415699	0.891292125700000
2	0.13832564467732045	0.13832564467730796	0.138325643800000
3	−0.7418168018560731	−0.7418168018560061	−0.741816797100000
4	−0.9399363018264509	−0.9399363018263659	−0.939936295800000
5	−0.2738827006359332	−0.2738827006359084	−0.273882698900000
6	0.6439773924444746	0.6439773924444164	0.643977388300000
7	0.9697676407653364	0.9697676407652488	0.969767634500000
8	0.4039579924791594	0.4039579924791229	0.403957989800000
9	−0.5332487711446274	−0.5332487711445792	−0.533248767700000
10	−0.9801890737807477	−0.9801890737806591	−0.980189067500000
x	Error for ETDM [22]	Error for MGMLFM	
0	$5.3012672040\times10^{-9}$	$7.460698725481052\times10^{-14}$	
1	$5.7285737890\times10^{-9}$	$8.060219158778636\times10^{-14}$	
2	$8.8905605100\times10^{-10}$	$1.249000902703301\times10^{-14}$	
3	$4.7678557200\times10^{-9}$	$6.705747068735946\times10^{-14}$	
4	$6.0412229310\times10^{-9}$	$8.504308368628699\times10^{-14}$	
5	$1.7603176390\times10^{-9}$	$2.475797344914099\times10^{-14}$	
6	$4.1390155720\times10^{-9}$	$5.81756864903582\times10^{-14}$	
7	$6.2329569540\times10^{-9}$	$8.759659664292485\times10^{-14}$	
8	$2.5963464570\times10^{-9}$	$3.652633751016765\times10^{-14}$	
9	$3.4273329990\times10^{-9}$	$4.818367926873179\times10^{-14}$	
10	$6.2999383020\times10^{-9}$	$8.85957973650875\times10^{-14}$	

In the same way as in Problem 4.3, we can express the approximate solution of Eq. (4.16) as in Eq. (4.13). Therefore, Eq. (4.16) can be rewritten in the following form:

$$\begin{aligned}
&\sum_{n=0}^{\infty}\big(-e^{x+y}\Lambda_1^{n+1}-e^{x+y}R_1^n\Gamma(n\alpha+1)+e^{x+y}R_2^n\Gamma(n\alpha+1)\big)\frac{t^{n\alpha}}{\Gamma(n\alpha+1)}\\
&=P+\sum_{n=0}^{\infty}K\bigg(\frac{\partial^2\big(-e^{x+y}\Lambda_1^n\big)}{\partial x^2}+\frac{\partial^2\big(-e^{x+y}\Lambda_1^n\big)}{\partial y^2}\bigg)\frac{t^{n\alpha}}{\Gamma(n\alpha+1)},\\
&\sum_{n=0}^{\infty}\big(e^{x+y}\Lambda_2^{n+1}-e^{x+y}R_3^n\Gamma(n\alpha+1)+e^{x+y}R_4^n\Gamma(n\alpha+1)\big)\frac{t^{n\alpha}}{\Gamma(n\alpha+1)}\\
&=-P+\sum_{n=0}^{\infty}K\bigg(\frac{\partial^2\big(e^{x+y}\Lambda_2^n\big)}{\partial x^2}+\frac{\partial^2\big(e^{x+y}\Lambda_2^n\big)}{\partial y^2}\bigg)\frac{t^{n\alpha}}{\Gamma(n\alpha+1)},
\end{aligned}\tag{4.19}$$

where

$$R_1^n=\sum_{k=0}^{n}\frac{\Lambda_1^k\partial\big(-e^{x+y}\Lambda_1^{n-k}\big)/\partial x}{\Gamma(k\alpha+1)\Gamma\big((n-k)\alpha+1\big)},$$

$$R_2^n = \sum_{k=0}^{n} \frac{\Lambda_2^k \partial\big(-e^{x+y}\Lambda_1^{n-k}\big)/\partial y}{\Gamma(k\alpha+1)\Gamma\big((n-k)\alpha+1\big)},$$
$$R_3^n = \sum_{k=0}^{n} \frac{\Lambda_1^k \partial\big(e^{x+y}\Lambda_2^{n-k}\big)/\partial x}{\Gamma(k\alpha+1)\Gamma\big((n-k)\alpha+1\big)},$$
$$R_4^n = \sum_{k=0}^{n} \frac{\Lambda_2^k \partial\big(e^{x+y}\Lambda_2^{n-k}\big)/\partial y}{\Gamma(k\alpha+1)\Gamma\big((n-k)\alpha+1\big)}.$$

When $n = 0$, we have

$$\Lambda_1^1 = \frac{1}{-e^{x+y}}\left(P + K\left[\frac{\partial^2\big(-e^{x+y}\Lambda_1^0\big)}{\partial x^2} + \frac{\partial^2\big(-e^{x+y}\Lambda_1^0\big)}{\partial y^2}\right] + e^{x+y}\big[R_1^0 + R_2^0\big]\right),$$
$$\Lambda_2^1 = \frac{1}{e^{x+y}}\left(-P + K\left[\frac{\partial^2\big(e^{x+y}\Lambda_2^0\big)}{\partial x^2} + \frac{\partial^2\big(e^{x+y}\Lambda_2^0\big)}{\partial y^2}\right] + e^{x+y}\big[R_3^0 + R_4^0\big]\right).$$

Then, for $n \geq 1$ the recursive relationships are given by

$$\begin{aligned}
\Lambda_1^{n+1} &= \frac{1}{-e^{x+y}}\left(K\left[\frac{\partial^2\big(-e^{x+y}\Lambda_1^n\big)}{\partial x^2} + \frac{\partial^2\big(-e^{x+y}\Lambda_1^n\big)}{\partial y^2}\right] + e^{x+y}\big[R_1^n + R_2^n\big]\Gamma(n\alpha+1)\right),\\
\Lambda_2^{n+1} &= \frac{1}{e^{x+y}}\left(K\left[\frac{\partial^2\big(e^{x+y}\Lambda_2^n\big)}{\partial x^2} + \frac{\partial^2\big(e^{x+y}\Lambda_2^n\big)}{\partial y^2}\right] + e^{x+y}\big[R_3^n + R_4^n\big]\Gamma(n\alpha+1)\right).
\end{aligned} \tag{4.20}$$

We can obtain the coefficients Λ_1^{n+1} and Λ_2^{n+1} by replacing $n = 1, 2, \ldots$. Then, we substitute these coefficients in the suggested solution in Eq. (4.13) to get the solution of Eq. (4.16).

The simulation of Problem 4.4 is illustrated in the following figures and tables. Figs. 4.12 and 4.14 presents the behavior of fractional-order solution obtained by GMLFM at $\alpha = 1$ for $U(x, y, t)$ and $V(x, y, t)$, respectively, and compared with their exact solution and display

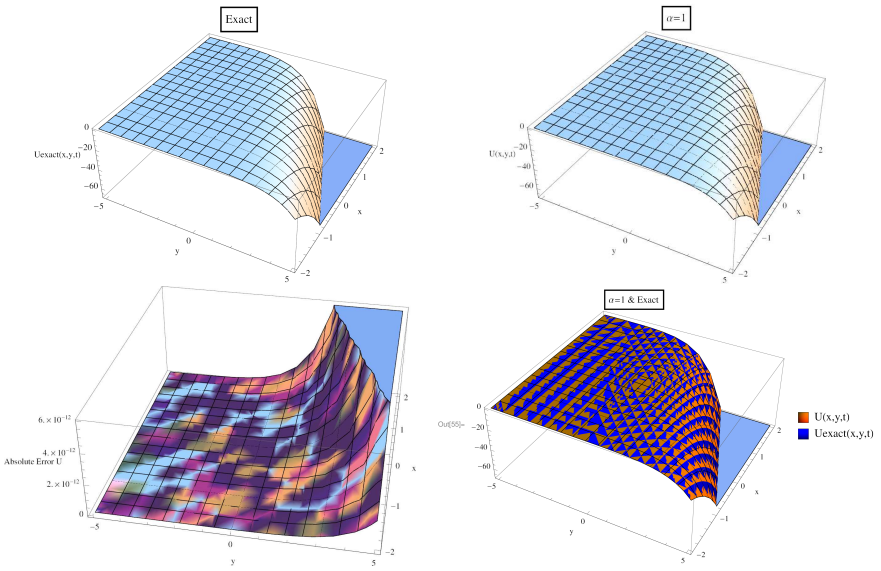

Fig. 4.12. The MGMLFM approximate solution of $U(x, y, t)$ when $\alpha = 1$, exact solution and absolute errors for Problem 4.4.

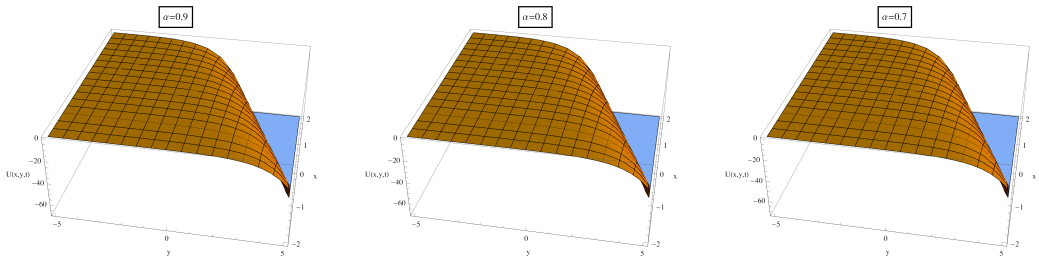

Fig. 4.13. The MGMLFM approximate solutions of $U(x, y, t)$ for Problem 4.4 with different values of α.

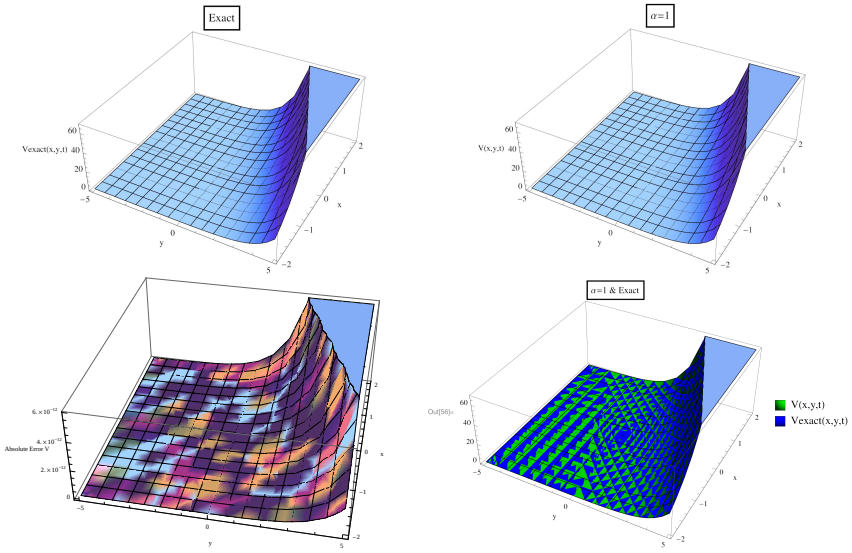

Fig. 4.14. The MGMLFM approximate solution of $V(x, y, t)$ when $\alpha = 1$, exact solution and absolute errors for Problem 4.4.

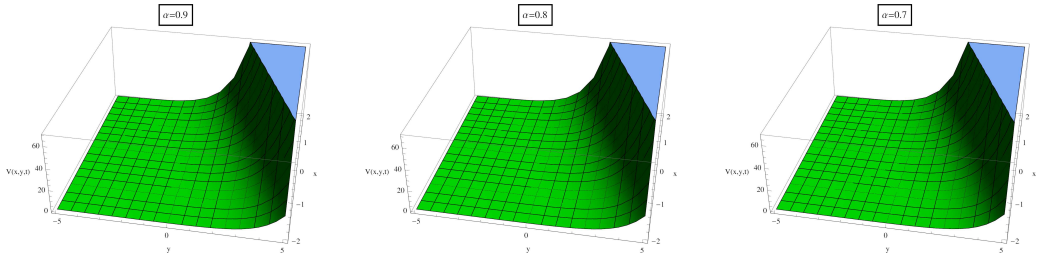

Fig. 4.15. The MGMLFM approximate solutions of $V(x, y, t)$ for Problem 4.4 with different values of α.

associated GMLFM absolute error. The impact of α on the behavior of the solution of $U(x, y, t)$ and $V(x, y, t)$, when α takes various values is displayed in Figs. 4.13 and 4.15, respectively. Moreover, two-dimensional plots at various values of α. In addition, two-dimensional drawings at various values of α are presented in Fig. 4.16 with respect to x and held y and t, in Fig. 4.17 they are drawn with t and fix x and y. The numerical values of the approximate solution gained from this method are compared with the exact solution in Tables 4.3 and 4.4, also, their absolute error is calculated.

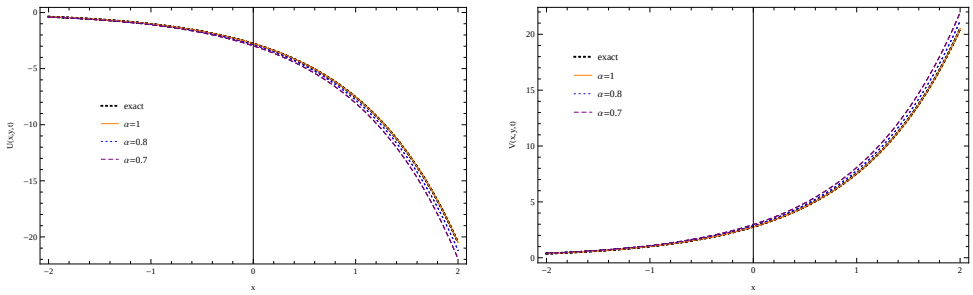

Fig. 4.16. The MGMLFM approximate solutions for $U(x, y, t)$ and $V(x, y, t)$ with x of Problem 4.4 when α takes various values, $y = 1$ and $t = 0.01$.

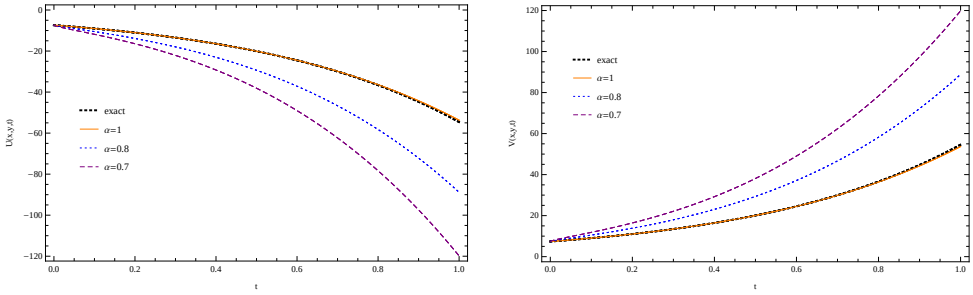

Fig. 4.17. The MGMLFM approximate solutions for $U(x, y, t)$ and $V(x, y, t)$ with t of Problem 4.4, when α takes various values, $y = 1$ and $x = 1$.

Table 4.3: The comparison of the exact solutions, outcomes obtained by MGMLFM and absolute errors for $U(x, y, t)$ of Problem 4.4 with different values of x at $t = 0.01$, $\alpha = 1$ and $y = 1$.

x	Exact	MGMLFM	Absolute Error for MGMLFM
0	−2.7731947639642978	−2.7731947639640557	$2.420286193682841\times10^{-13}$
1	−7.538324933661922	−7.538324933661264	$6.581402089977928\times10^{-13}$
2	−20.49129168419294	−20.49129168419115	$1.790567694115452\times10^{-12}$
3	−55.70110582679559	−55.70110582679075	$4.838796030526282\times10^{-12}$
4	−151.41130379405269	−151.41130379403953	$1.315925146627705\times10^{-11}$
5	−411.5785957266655	−411.57859572662977	$3.575451046344824\times10^{-11}$
6	−1118.7866177464866	−1118.7866177463893	$9.731593308970332\times10^{-11}$
7	−3041.1773329434304	−3041.177332943166	$2.642082108650356\times10^{-10}$
8	−8266.77708126167	−8266.777081260952	$7.185008144006133\times10^{-10}$
9	−22471.429919915303	−22471.429919913353	$1.949956640601158\times10^{-9}$
10	−61083.679610796666	−61083.67961079136	$5.304173100739717\times10^{-9}$

The results presented in the previous figures and tables confirmed that the approximate fractional solution is in complete agreement with the exact solution and the error rate is very small, which confirms the higher accuracy and efficiency of the used method.

Table 4.4: The comparison of the exact solutions, outcomes obtained by MGMLFM and absolute errors for $V(x,y,t)$ of Problem 4.4 with different values of x at $t=0.01$, $\alpha=1$ and $y=1$.

x	Exact	MGMLFM	Absolute Error for MGMLFM
0	2.7731947639642978	2.7731947639640557	$2.420286193682841\times10^{-13}$
1	7.538324933661922	7.538324933661264	$6.581402089977928\times10^{-13}$
2	20.49129168419294	20.49129168419115	$1.790567694115452\times10^{-12}$
3	55.70110582679559	55.70110582679075	$4.838796030526282\times10^{-12}$
4	151.41130379405269	151.41130379403953	$1.315925146627705\times10^{-11}$
5	411.5785957266655	411.57859572662977	$3.575451046344824\times10^{-11}$
6	1118.7866177464866	1118.7866177463893	$9.731593308970332\times10^{-11}$
7	3041.1773329434304	3041.177332943166	$2.642082108650356\times10^{-10}$
8	8266.77708126167	8266.777081260952	$7.185008144006133\times10^{-10}$
9	22471.429919915303	22471.429919913353	$1.949956640601158\times10^{-9}$
10	61083.679610796666	61083.67961079136	$5.304173100739717\times10^{-9}$

Problem 4.5. Consider the three-dimensional time fractional-order NSE

$$\begin{aligned}
&{}_0^C D_t^\alpha U + U\frac{\partial U}{\partial x} + V\frac{\partial U}{\partial y} + W\frac{\partial U}{\partial z} = K\left[\frac{\partial^2 U}{\partial x^2} + \frac{\partial^2 U}{\partial y^2} + \frac{\partial^2 U}{\partial z^2}\right] + P_1,\\
&{}_0^C D_t^\alpha V + U\frac{\partial V}{\partial x} + V\frac{\partial V}{\partial y} + W\frac{\partial V}{\partial z} = K\left[\frac{\partial^2 V}{\partial x^2} + \frac{\partial^2 V}{\partial y^2} + \frac{\partial^2 V}{\partial z^2}\right] - P_2,\\
&{}_0^C D_t^\alpha W + U\frac{\partial W}{\partial x} + V\frac{\partial W}{\partial y} + W\frac{\partial W}{\partial z} = K\left[\frac{\partial^2 W}{\partial x^2} + \frac{\partial^2 W}{\partial y^2} + \frac{\partial^2 W}{\partial z^2}\right] - P_3
\end{aligned} \tag{4.21}$$

with the associated ICs

$$\begin{aligned}
&U(x,y,z,0) = U_0 = -0.5x + y + z,\\
&V(x,y,z,0) = V_0 = x - 0.5y + z,\\
&W(x,y,z,0) = W_0 = x + y - 0.5z.
\end{aligned} \tag{4.22}$$

In the particular case when $\alpha = 1$ the exact solution [14, 36] is given by

$$\begin{aligned}
U(x,y,z,t) &= \frac{-0.5x + y + z - 2.25xt}{1 - 2.25t^2},\\
V(x,y,z,t) &= \frac{x - 0.5y + z - 2.25yt}{1 - 2.25t^2},\\
W(x,y,z,t) &= \frac{x + y - 0.5z - 2.25zt}{1 - 2.25t^2}.
\end{aligned} \tag{4.23}$$

Following the analysis of the MGMLFM presented in Section 3, we assume that the solution of Eq.(4.21) is given by

$$\begin{aligned}
U(x,y,z,t) &= \Upsilon_1(x,y,z)E_\alpha\left(\Lambda_1 t^\alpha\right) = \sum_{n=0}^{\infty}\Upsilon_1(x,y,z)\Lambda_1^n\frac{t^{n\alpha}}{\Gamma(n\alpha+1)},\\
V(x,y,z,t) &= \Upsilon_2(x,y,z)E_\alpha\left(\Lambda_2 t^\alpha\right) = \sum_{n=0}^{\infty}\Upsilon_2(x,y,z)\Lambda_2^n\frac{t^{n\alpha}}{\Gamma(n\alpha+1)},\\
W(x,y,z,t) &= \Upsilon_3(x,y,z)E_\alpha\left(\Lambda_3 t^\alpha\right) = \sum_{n=0}^{\infty}\Upsilon_3(x,y,z)\Lambda_3^n\frac{t^{n\alpha}}{\Gamma(n\alpha+1)},
\end{aligned} \tag{4.24}$$

where Λ_1, Λ_2 and Λ_3 are undetermined coefficients. From Eq. (4.23) we have

$$\Upsilon_1(x,y,z) = U_0, \quad \Upsilon_2(x,y,z) = V_0, \quad \Upsilon_3(x,y,z) = W_0.$$

According to the analysis of MGMLFM presented in Section 3, Eq. (4.21) can be rewritten as follows:

$$\begin{aligned}
&\sum_{n=0}^{\infty}\bigg(U_0\Lambda_1^{n+1} + U_0C_1^n\Gamma(n\alpha+1) + V_0C_2^n\Gamma(n\alpha+1) + W_0C_3^n\Gamma(n\alpha+1)\\
&\qquad - K\frac{\partial^2(U_0\Lambda_1^n)}{\partial x^2} - K\frac{\partial^2(U_0\Lambda_1^n)}{\partial y^2} - K\frac{\partial^2(U_0\Lambda_1^n)}{\partial z^2}\bigg)\frac{t^{n\alpha}}{\Gamma(n\alpha+1)} = P_1,\\
&\sum_{n=0}^{\infty}\bigg(V_0\Lambda_2^{n+1} + U_0C_4^n\Gamma(n\alpha+1) + V_0C_5^n\Gamma(n\alpha+1) + W_0C_6^n\Gamma(n\alpha+1)\\
&\qquad - K\frac{\partial^2(V_0\Lambda_2^n)}{\partial x^2} - K\frac{\partial^2(V_0\Lambda_2^n)}{\partial y^2} - K\frac{\partial^2(V_0\Lambda_2^n)}{\partial z^2}\bigg)\frac{t^{n\alpha}}{\Gamma(n\alpha+1)} = P_2,\\
&\sum_{n=0}^{\infty}\bigg(W_0\Lambda_3^{n+1} + U_0C_7^n\Gamma(n\alpha+1) + V_0C_8^n\Gamma(n\alpha+1) + W_0C_9^n\Gamma(n\alpha+1)\\
&\qquad - K\frac{\partial^2(W_0\Lambda_3^n)}{\partial x^2} - K\frac{\partial^2(W_0\Lambda_3^n)}{\partial y^2} - K\frac{\partial^2(W_0\Lambda_3^n)}{\partial z^2}\bigg)\frac{t^{n\alpha}}{\Gamma(n\alpha+1)} = -P_3,
\end{aligned} \tag{4.25}$$

where

$$\begin{aligned}
C_1^n &= \sum_{k=0}^{n}\frac{\Lambda_1^k\partial\big(U_0\Lambda_1^{n-k}\big)/\partial x}{\Gamma(k\alpha+1)\Gamma\big((n-k)\alpha+1\big)}, \quad C_2^n = \sum_{k=0}^{n}\frac{\Lambda_2^k\partial\big(U_0\Lambda_1^{n-k}\big)/\partial y}{\Gamma(k\alpha+1)\Gamma\big((n-k)\alpha+1\big)},\\
C_3^n &= \sum_{k=0}^{n}\frac{\Lambda_3^k\partial\big(U_0\Lambda_1^{n-k}\big)/\partial z}{\Gamma(k\alpha+1)\Gamma\big((n-k)\alpha+1\big)}, \quad C_4^n = \sum_{k=0}^{n}\frac{\Lambda_1^k\partial\big(V_0\Lambda_2^{n-k}\big)/\partial x}{\Gamma(k\alpha+1)\Gamma\big((n-k)\alpha+1\big)},\\
C_5^n &= \sum_{k=0}^{n}\frac{\Lambda_2^k\partial\big(V_0\Lambda_2^{n-k}\big)/\partial y}{\Gamma(k\alpha+1)\Gamma\big((n-k)\alpha+1\big)}, \quad C_6^n = \sum_{k=0}^{n}\frac{\Lambda_3^k\partial\big(V_0\Lambda_2^{n-k}\big)/\partial z}{\Gamma(k\alpha+1)\Gamma\big((n-k)\alpha+1\big)},\\
C_7^n &= \sum_{k=0}^{n}\frac{\Lambda_1^k\partial\big(W_0\Lambda_3^{n-k}\big)/\partial x}{\Gamma(k\alpha+1)\Gamma\big((n-k)\alpha+1\big)}, \quad C_8^n = \sum_{k=0}^{n}\frac{\Lambda_2^k\partial\big(W_0\Lambda_3^{n-k}\big)/\partial y}{\Gamma(k\alpha+1)\Gamma\big((n-k)\alpha+1\big)},\\
C_9^n &= \sum_{k=0}^{n}\frac{\Lambda_3^k\partial\big(W_0\Lambda_3^{n-k}\big)/\partial z}{\Gamma(k\alpha+1)\Gamma\big((n-k)\alpha+1\big)}.
\end{aligned}$$

When $n = 0$, we have

$$\begin{aligned}
\Lambda_1^1 &= \frac{1}{U_0}\bigg(P_1 + K\bigg[\frac{\partial^2\big(U_0\Lambda_1^0\big)}{\partial x^2} + \frac{\partial^2\big(U_0\Lambda_1^0\big)}{\partial y^2} + \frac{\partial^2\big(U_0\Lambda_1^0\big)}{\partial z^2}\bigg] - \big[U_0C_1^0 + V_0C_2^0 + W_0C_3^0\big]\bigg),\\
\Lambda_2^1 &= \frac{1}{V_0}\bigg(P_2 + K\bigg[\frac{\partial^2\big(V_0\Lambda_2^0\big)}{\partial x^2} + \frac{\partial^2\big(V_0\Lambda_2^0\big)}{\partial y^2} + \frac{\partial^2\big(V_0\Lambda_2^0\big)}{\partial z^2}\bigg] - \big[U_0C_4^0 + V_0C_5^0 + W_0C_6^0\big]\bigg),\\
\Lambda_3^1 &= \frac{1}{W_0}\bigg(-P_3 + K\bigg[\frac{\partial^2(W_0\Lambda_3^0)}{\partial x^2} + \frac{\partial^2\big(W_0\Lambda_3^0\big)}{\partial y^2} + \frac{\partial^2\big(W_0\Lambda_3^0\big)}{\partial z^2}\bigg] - \big[U_0C_7^0 + V_0C_8^0 + W_0C_9^0\big]\bigg).
\end{aligned} \tag{4.26}$$

Therefore, from Eq. (4.25) the recurrence relation is given as the following:

$$\Lambda_1^{n+1} = \frac{1}{U_0}\bigg(K\bigg[\frac{\partial^2\big(U_0\Lambda_1^n\big)}{\partial x^2} + \frac{\partial^2\big(U_0\Lambda_1^n\big)}{\partial y^2} + \frac{\partial^2\big(U_0\Lambda_1^n\big)}{\partial z^2}\bigg] \tag{4.27a}$$

$$- \left[U_0 C_1^n + V_0 C_2^n + W_0 C_3^n\right]\Gamma(n\alpha+1)\Big), \tag{4.27b}$$

$$\Lambda_2^{n+1} = \frac{1}{V_0}\Bigg(K\left[\frac{\partial^2\left(V_0\Lambda_2^n\right)}{\partial x^2} + \frac{\partial^2\left(V_0\Lambda_2^n\right)}{\partial y^2} + \frac{\partial^2\left(V_0\Lambda_2^n\right)}{\partial z^2}\right] \tag{4.27c}$$

$$- \left[U_0 C_4^n + V_0 C_5^n + W_0 C_6^n\right]\Gamma(n\alpha+1)\Big), \tag{4.27d}$$

$$\Lambda_3^{n+1} = \frac{1}{W_0}\Bigg(K\left[\frac{\partial^2\left(W_0\Lambda_3^n\right)}{\partial x^2} + \frac{\partial^2\left(W_0\Lambda_3^n\right)}{\partial y^2} + \frac{\partial^2\left(W_0\Lambda_3^n\right)}{\partial z^2}\right] \tag{4.27e}$$

$$- \left[U_0 C_7^n + V_0 C_8^n + W_0 C_9^n\right]\Gamma(n\alpha+1)\Big). \tag{4.27f}$$

Then, we can get coefficients of the solution (4.24) from the recurrence relation (4.27) by substituting various values of n ($n \geq 1$) in order to obtain the components the following series:

$$U(x,y,z,t) = U_0\left(\Lambda_1^0 + \Lambda_1^1\frac{t^\alpha}{\Gamma(\alpha+1)} + \Lambda_1^2\frac{t^{2\alpha}}{\Gamma(2\alpha+1)} + \Lambda_1^3\frac{t^{3\alpha}}{\Gamma(3\alpha+1)} + \cdots\right),$$
$$V(x,y,z,t) = V_0\left(\Lambda_2^0 + \Lambda_2^1\frac{t^\alpha}{\Gamma(\alpha+1)} + \Lambda_2^2\frac{t^{2\alpha}}{\Gamma(2\alpha+1)} + \Lambda_2^3\frac{t^{3\alpha}}{\Gamma(3\alpha+1)} + \cdots\right),$$
$$W(x,y,z,t) = W_0\left(\Lambda_3^0 + \Lambda_3^1\frac{t^\alpha}{\Gamma(\alpha+1)} + \Lambda_3^2\frac{t^{2\alpha}}{\Gamma(2\alpha+1)} + \Lambda_3^3\frac{t^{3\alpha}}{\Gamma(3\alpha+1)} + \cdots\right).$$

The behavior of approximate fractional solution for the Problem 4.5 is displayed in Figs. 4.18-4.23. In Fig. 4.18, we show the comparison between the approximate fractional solution given by MGMLFM with the exact solution for Eq. (4.21) using ICs Eq. (4.22). The behavior of the approximate solution when α takes various values for $U(x,y,z,t), V(x,y,z,t)$ and $W(x,y,z,t)$ is shown in Figs. 4.19-4.21, respectively, as well as the two-dimensional graphs at various values of α with respect to state x and time t are presented in Figs. 4.22 and 4.23, respectively.

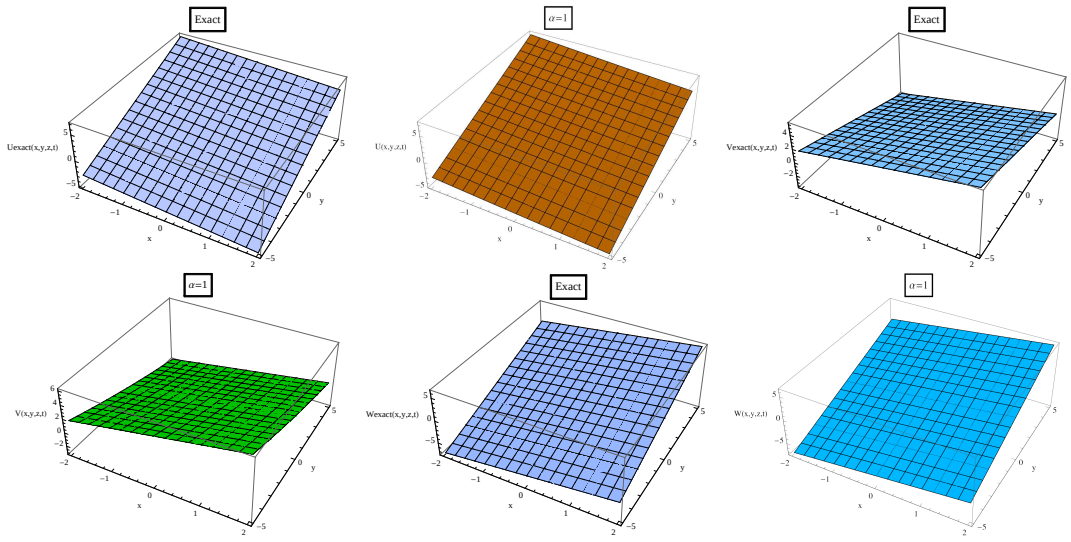

Fig. 4.18. The compression of MGMLFM approximate solutions for Problem 4.5 when $\alpha = 1$ with exact solutions.

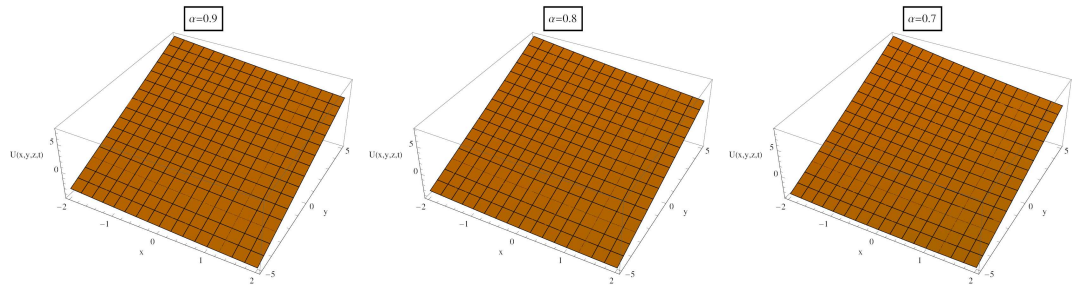

Fig. 4.19. The MGMLFM approximate solutions of $U(x, y, z, t)$ for Problem 4.5 with various values of α.

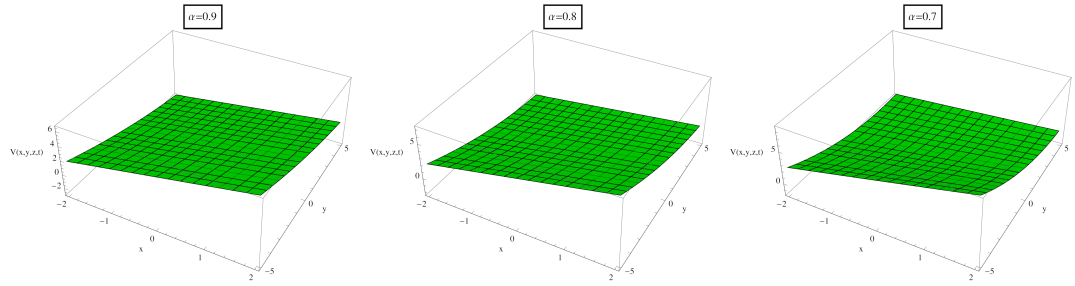

Fig. 4.20. The MGMLFM approximate solutions of $V(x, y, z, t)$ for Problem 4.5 with various values of α.

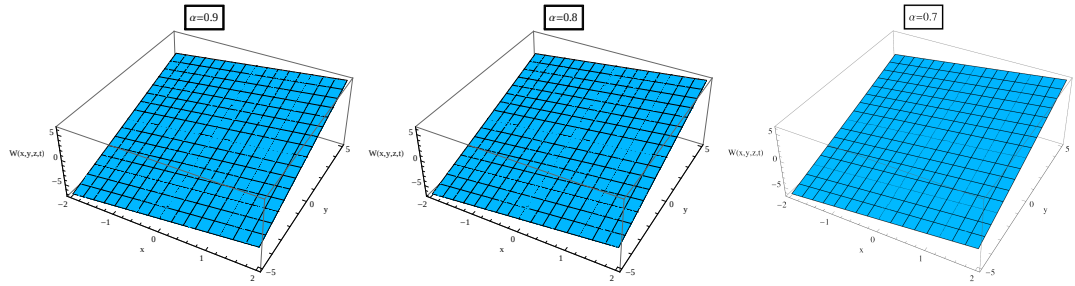

Fig. 4.21. The MGMLFM approximate solutions of $W(x, y, z, t)$ for Problem 4.5 with various values of α.

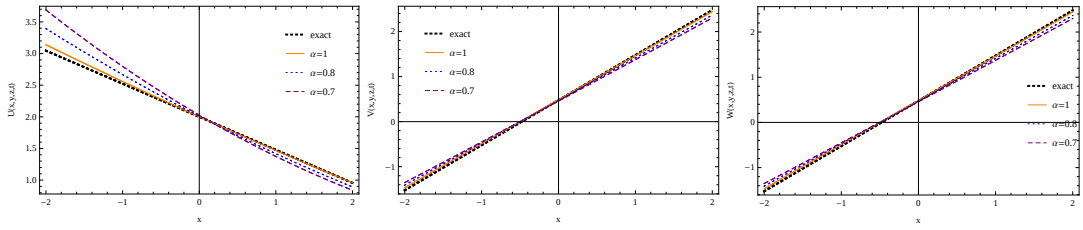

Fig. 4.22. The MGMLFM approximate solutions of $U(x, y, z, t), V(x, y, z, t)$ and $W(x, y, z, t)$ with x for Problem 4.5, when α takes various values, $y = 0.5, z = 1$ and $t = 0.01$.

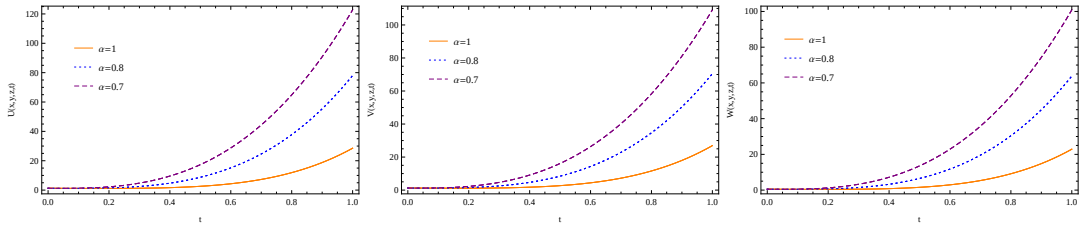

Fig. 4.23. The MGMLFM approximate solutions of $U(x,y,z,t), V(x,y,z,t)$ and $W(x,y,z,t)$ with t for Problem 4.5, when α takes various values, $y = 0.5, x = 0.5$ and $z = 1$.

5. Conclusion

In this paper, we adopted a newly developed method namely MGMLFM to obtain the approximate analytical solution of some nonlinear time-fractional multi-dimensional NSEs. The mathematical formalism for the proposed problem depended on the sense of CFD. Approximate solutions were provided in power series form. We carried out the current method on five problems to illustrate the validity and efficiency of this method. The numerical simulation for gained results was presented in some two and three-dimensional figures. We introduced a comparison between our results with known exact solutions, where it was found the fractional-order solutions convergence towards integer-order solutions (i.e. exact solutions) when $\alpha = 1$. Also, solutions in different fractional orders were specified and found to be interesting in terms of explaining the different dynamic behaviors of the proposed problems. Moreover, the numerical values of the results obtained with MGMLFM were presented in some tables and compared with the known exact solutions and the solutions obtained by other methods in the literature under the same conditions, and their absolute errors were also presented. The performed calculations in this research confirmed the accuracy, efficiency and suitability of the MGMLFM for solving such types of models. The advantages of the proposed method are straightforward, requires small efforts of computation, simple procedures, convergence quickly to exact solutions and does not require any perturbation, discretization and transformation unlike some other methods. Therefore, we suggest this method to solve other linear and nonlinear models of fractional order that have applications in engineering, science and physical phenomena.

References

[1] H.M. Ali, New approximate solutions to fractional smoking model using the generalized Mittag-Leffler function method, *Prog. Fract. Differ. Appl.*, **5**:4 (2019), 319–326.

[2] H.M. Ali, An efficient approximate-analytical method to solve time-fractional KdV and KdVB equations, *Inf. Sci. Lett.*, **9**:3 (2020), 189–198.

[3] H.M. Ali, H. Ahmad, S. Askar, and I.G. Ameen, Efficient approaches for solving systems of nonlinear time-fractional partial differential equations, *Fractal Fract.*, **6**:1 (2022), 32.

[4] H.M. Ali, K.S. Nisar, W.R. Alharbi, and M. Zakarya, Efficient approximate analytical technique to solve nonlinear coupled Jaulent-Miodek system within a time-fractional order, *AIMS Math.*, **9**:3 (2024), 5671–5685.

[5] I.G. Ameen, H.M. Ali, M.R. Alharthi, A.H. Abdel-Aty, and H.M. Elshehabey, Investigation of the dynamics of COVID-19 with a fractional mathematical model: A comparative study with actual data, *Results Phys.*, **23** (2021), 103976.

[6] I.G. Ameen, N. Sweilam, and H.M. Ali, A fractional-order model of human liver: Analytic-approximate and numerical solutions comparing with clinical data, *Alexandria Eng. J.*, **60** (2021), 4797–4808.

[7] I.G. Ameen, R.O.A. Taie, and H.M. Ali, Two effective methods for solving nonlinear coupled time-fractional Schrödinger equations, *Alexandria Eng. J.*, **70** (2023), 331–347.

[8] A.A.M. Arafa, S.Z. Rida, A.A. Mohammadein, and H.M. Ali, Solving nonlinear fractional differential equation by generalized Mittag-Leffler function method, *Commun. Theor. Phys.*, **59**:6 (2013), 661–663.

[9] F. Ayaz and K. Heredağ, Fractional model for blood flow under MHD influence in porous and non-porous media, *Int. J. Optim. Control. Theor. Appl. IJOCTA*, **14**:2 (2024), 156–167.

[10] D. Baleanu, K. Diethelm, E. Scalas, and J.J. Trujillo, *Fractional Calculus: Models and Numerical Methods*, in: *Series on Complexity, Nonlinearity and Chaos*, Vol. 3, World Scientific Publishing Company, 2012.

[11] M. Bilal, S. Rehman, and J. Ahmad, The study of new optical soliton solutions to the time-space fractional nonlinear dynamical model with novel mechanisms, *J. Ocean Eng. Sci.*, 2022. https://doi.org/10.1016/j.joes.2022.05.027

[12] D.W. Brzeziński, Comparison of fractional order derivatives computational accuracy – right hand vs left hand definition, *Appl. Math. Nonlinear Sci.*, **2**:1 (2017), 237–248.

[13] C. Cattani, H.M. Srivastava, and X.J. Yang, *Fractional Dynamics*, de Gruyter Open, 2015.

[14] Y.M. Chu, N. Ali Shah, P. Agarwal, and J. Dong Chung, Analysis of fractional multi-dimensional Navier-Stokes equation, *Adv. Differential Equations*, **2021**:1 (2021), 91.

[15] M. Cinar, I. Onder, A. Secer, M. Bayram, T. Abdulkadir Sulaiman, and A. Yusuf, Solving the fractional Jaulent-Miodek system via a modified Laplace decomposition method, *Waves Random Complex Media*, **2022** (2022). https://doi.org/10.1080/17455030.2022.2057613

[16] E.M. Elsayed, R. Shah, and K. Nonlaopon, The analysis of the fractional-order Navier-Stokes equations by a novel approach, *J. Funct. Spaces*, **2022**:1 (2022), 8979447.

[17] M. El-Shahed and A. Salem, On the generalized Navier-Stokes equations, *Appl. Math. Comput.*, **156**:1 (2005), 287–293.

[18] A. Ghorbani, Beyond Adomian polynomials: He polynomials, *Chaos Solitons Fractals*, **39** (2009), 1486–1492.

[19] C. Han, Y. Cheng, R. Ma, and Z. Zhao, Average process of fractional Navier-Stokes equations with singularly oscillating force, *Fractal Fract.*, **6**:5 (2022), 241.

[20] K.K. Jaber and R.S. Ahmad, Analytical solution of the time fractional Navier-Stokes equation, *Ain Shams Eng. J.*, **9**:4 (2018), 1917–1927.

[21] R.M. Jena and S. Chakraverty, Solving time-fractional Navier-Stokes equations using homotopy perturbation Elzaki transform, *SN Appl. Sci.*, **1** (2019), 16.

[22] H. Khan, A. Khan, P. Kumam, D. Baleanu, and M. Arif, An approximate analytical solution of the Navier-Stokes equations within Caputo operator and Elzaki transform decomposition method, *Adv. Differential Equations*, **2020** (2020), 622.

[23] H. Khan, Q. Khan, P. Kumam, F. Tchier, S. Ahmed, G. Singh, and K. Sitthithakerngkiet, The fractional view analysis of the Navier-Stokes equations within Caputo operator, *Chaos Solitons Fractals:X*, **8** (2022), 100076.

[24] A.A. Kilbas, H.M. Srivastava, and J.J. Trujillo, *Theory and Applications of Fractional Differential Equations*, Elsevier, 2006.

[25] D. Kumar, J. Singh, and S. Kumar, A fractional model of Navier-Stokes equation arising in unsteady flow of a viscous fluid, *J. Assoc. Arab Univ. Basic Appl. Sci.*, **17** (2015), 14–19.

[26] D. Kumar, J. Singh, K. Tanwar, and D. Baleanu, A new fractional exothermic reactions model having constant heat source in porous media with power, exponential and Mittag-Leffler laws, *Int. J. Heat Mass Transf.*, **138** (2019), 1222–1227.

[27] S. Kumar, A. Kumar, S. Abbas, M. Al Qurashi, and D. Baleanu, A modified analytical approach

with existence and uniqueness for fractional Cauchy reaction-diffusion equations, *Adv. Differential Equations*, **2020** (2020), 28.

[28] Y. Liu, H. Sun, X. Yin, and B. Xin, A new Mittag-Leffler function undetermined coefficient method and its applications to fractional homogeneous partial differential equations, *J. Nonlinear Sci. Appl.*, **10**:8 (2017), 4515–4523.

[29] R.L. Magin, *Fractional Calculus in Bioengineering*, Vol. 2, Begell House Redding, 2006.

[30] A.M.S. Mahdy, N.H. Sweilam, and M. Higazy, Approximate solution for solving nonlinear fractional order smoking model, *Alexandria Eng. J.*, **59** (2020), 739–752.

[31] I. Masti, K. Sayevand, and H. Jafari, On analyzing two dimensional fractional order brain tumor model based on orthonormal Bernoulli polynomials and Newton's method, *Int. J. Optim. Control. Theor. Appl. IJOCTA*, **14**:1 (2024), 12–19.

[32] S.T. Mohyud-Din, M.A. Noor, and K.I. Noor, Traveling wave solutions of seventh-order generalized KdV equations using he's polynomials, *Int. J. Nonlinear Sci. Numer. Simul.*, **10** (2009), 227–233.

[33] S. Momani and Z. Odibat, Analytical solution of a time-fractional Navier-Stokes equation by Adomian decomposition method, *Appl. Math. Comput.*, **177** (2006), 488–494.

[34] C.L.M.H. Navier, Memoire sur les lois du mouvement des fluides, *Mem. Acad. Sci. Inst. France*, **6** (1822), 389–440.

[35] I. Podlubny, *Fractional Differential Equations: An Introduction to Fractional Derivatives, Fractional Differential Equations, to Methods of Their Solution and Some of Their Applications*, in: *Mathematics in Science and Engineering*, Vol. 198, Academic Press, 1999.

[36] B.K. Singh and P. Kumar, FRDTM for numerical simulation of multi-dimensional, time-fractional model of Navier–Stokes equation, *Ain Shams Eng. J.*, **9**:4 (2018), 827–834.

[37] J. Singh, D. Kumar, and D. Baleanu, New aspects of fractional Biswas-Milovic model with Mittag-Leffler law, *Math. Model. Nat. Phenom.*, **14**:3 (2019), 303.

[38] M. Yavuz and N. Özdemir, Numerical inverse Laplace homotopy technique for fractional heat equations, *Therm. Sci.*, **22**:1 (2018), 185–194.

[39] M. Yavuz and N. Özdemir, European vanilla option pricing model of fractional order without singular kernel, *Fractal Fract.*, **2**:1 (2018), 3.

[40] Y. Zhou and L. Peng, Weak solutions of the time-fractional Navier-Stokes equations and optimal control, *Comput. Math. Appl.*, **73** (2017), 1016–1027.